Chang et al. BMC Zoology (2020) 5:15
https://doi.org/10.1186/s40850-020-00064-4

BMC Zoology

RESEARCH ARTICLE Open Access

Investigation of epididymal proteins and general sperm membrane characteristics of Formosan pangolin (*Manis pentadactyla pentadactyla*)

Yu-Chia Chang[1,2†], Jane-Fang Yu[1,3†], Tse-En Wang[2], Shih-Chien Chin[3], Yu-Syuan Wei[2,4], Ting-Yu Chen[3] and Pei-Shiue Tsai[2,4,5*]

Abstract

Background: Formosan Pangolin (*Manis pentadactyla pentadactyla*) is one of the three subspecies of Chinese pangolins, it is also an isolated sub-species naturally habitat in Taiwan. Despite earlier report on successful breeding of Sunda (*Manis javanica*) pangolin, breeding of Formosan pangolins in zoo captive populations is still challenging due to unknown reproductive characterizations of this species in both male and female populations.

Results: We characterized for the first time, reproductive tract of male Formosan pangolin. We showed pangolin epididymis was a collagen-enriched organ with apparent segmented sub-regions similar to other mammals. However, unlike most mammals exhibited two V-ATPase subunits, Formosan pangolin exhibited only V-ATPase subunit 2. This specific V-ATPase subunit extended its cellular localization throughout the cytoplasm of epididymal clear cells, suggesting pH regulation of luminal microenvironment might be different from other mammals. Electron micrographs showed rod-shaped pangolin sperm cells with multi-lamellar membrane structure at the sperm head. Similar to well-defined capacitation and acrosome reaction membrane changes in other mammals, we reported three distinct patterns (homogenous, punctuated and faded) of pangolin sperm head membrane changes. The concurrent increase in phosphotyrosine protein expression detected at the sperm mid-piece/tail and the emergence of punctuated membrane aggregates likely representing three sperm activation stages, namely inactivated, capacitated and acrosome reacted status of pangolin sperm.

Conclusion: By revealing unique epididymal V-ATPase distribution and sperm membrane dynamics in Formosan pangolin, we would understand better the fundamental aspects of reproduction parameters of Formosan pangolin.

Keywords: Pangolin, Epididymis, Sperm, Reproduction, V-ATPase

* Correspondence: psjasontsai@ntu.edu.tw
†Yu-Chia Chang and Jane-Fang Yu contributed equally to this work.
[2]Graduate Institute of Veterinary Medicine, National Taiwan University, No. 1, Sec. 4, Roosevelt Rd, 10617 Taipei, Taiwan
[4]Department of Veterinary Medicine, National Taiwan University, No. 1, Sec. 4, Roosevelt Rd, 10617 Taipei, Taiwan
Full list of author information is available at the end of the article

Background

Pangolins belong to Manidae family under the mammalian order Pholidota [1, 2]. They are nocturnal ants or termites- eating mammals and are mostly habit in tropical or subtropical countries. Currently, there are eight species of pangolin have been identified; however, knowledge regarding their reproductive biology is still limited, this is partially due to their nocturnal lifestyle and underground activities during the daylight and limited number of individuals to allow routine or frequent research evaluations as in other species. Moreover, destruction on their natural habitats with increasing illegal trading of pangolins substantially accelerate the decline of their population adding additional restricted factor for routine research purpose and evaluations. The Formosan Pangolin (*Manis pentadactyla pentadactyla; M. P. pentadactyla*) is one of the three subspecies of Chinese pangolins, and is an isolated subspecies habitats in Taiwan [3]. Based on international union for conservation of nature red list of threatened species (IUCN) published in 2015 and 2019, Chinese pangolin (*Manis pentadactyla*) has been listed in the category of critically endangered [4, 5]. Despite few reports stated the success on breeding Sunda (*Manis javanica*) pangolin [6], breeding of different Chinese pangolins sub-species in zoo captive populations had been less successful in the past decades [7, 8].

Raising different animal species including pangolin requires optimized breeding protocol covering various aspects including appropriate nutritional formulation, veterinary care and the most importantly, comprehensive understanding of both male and female pangolin reproductive physiology [7, 9]. In earlier study, we developed a progesterone-based radioimmunoassay to monitor the gestation period of rescued Formosan pangolin, from that study, we reported that during gestation, the serum progesterone of pregnant pangolins remained at 10–55 ng/ml with a peak at 47.6 ng/ml, whereas the serum progesterone of non-pregnant pangolins remained at 1.99 ± 1.62 ng/ml to 2.27 ± 1.64 ng/ml [10]. In addition, the gestation period of Formosan pangolins have been reported [10, 11]; however, information regarding basic male reproduction is almost absent. In this study, we characterized reproductive tract of male Formosan pangolin, and reported for the first time, epididymal structure and the presence of proteins that have been suggested to be critical for their roles on maintaining the homeostasis of male reproductive tract in other mammals. Understanding of male reproductive tract of Formosan pangolin will advance breeding success in zoo captive population and facilitate future preservation of pangolin sperm and allow repopulation of this endangered species.

Results

Detection of V-ATPase subunit B2, but not B1 in the clear cells of fibrotic tissue-enriched pangolin epididymis

As showed in Fig. 1a, we observed apparent compartmentalization of pangolin epididymis by connective tissue that separated initial segment, caput, corpus and cauda regions. In agreement with histological arrangement of other mammals, pangolin epididymal lumen was consisted of single layer of epithelial cells surrounded and formed the basic luminal structure (Fig. 1a). The diameters of the lumen were measured as 70.17 ± 18.9 μm, 89.87 ± 19.1 μm, 192.41 ± 39.2 μm, 257.36 ± 31.7 μm for initial segment, caput, corpus and cauda epididymis, respectively (Fig. 1b). Despite connective tissues were commonly observed to separate different regions of epididymis; however, when tissue section was subjected to Masson's trichrome stain which commonly used to identify fibrotic tissue, unlike in other species where connective tissue present mostly at the restricted regions between epididymal segments, we detected large amount of fibrotic tissue present within or surrounding the epididymis (Fig. 1c, stained in blue). To further compare physiological similarity or differences between pangolin epididymis with other mammals, we examined three typical epididymal proteins, vacuolar type H^+ – ATPase (V-ATPase), quiescin sulfhydryl oxidase 2 (QSOX2) and E-Cadherin which were known to present specifically in clear cells (V-ATPase) [12], principal cells (QSOX2) [13], or at the lateral membrane of epithelia (E-Cadherin); moreover, these proteins have been suggested to modulate the acidification of luminal microenvironment (V-ATPase), or to maintain luminal architecture (E-Cadherin) of the epididymis [12, 14]. In line with other studies [15, 16], we showed in Fig. 2a, mouse epididymal clear cells contained both V-ATPase subunit B1 (in red) and B2 (in green) (Fig. 2a, upper panel); although we also detected the presence of V-ATPase in pangolin epididymis; however, unlike mouse epididymis showed the presence of both subunits, pangolin epididymal epithelium exhibited only V-ATPase B2 subunit, but not B1 (Fig. 2a, lower panel). E-Cadherin is a adhesion junction protein known to present at the lateral membrane of the epithelium, the function of E-Cadherin is known to stabilize the polarized structure of the epithelia, in combination with QSOX2 protein that is known to present specifically in the principal cells, we showed in Fig. 2b, e-Cadherin and QSOX2 were present and localized at the expected cellular localization of the epididymal epithelium suggesting the basic luminal structure of pangolin epididymis was similar to most mammals (Fig. 2b).

Pangolin sperm exhibited avian-like rod-shaped sperm head with 9 + 2 axoneme containing flagella

As no current knowledge regarding sperm cells of ant-eating mammals is available, we next analysed the

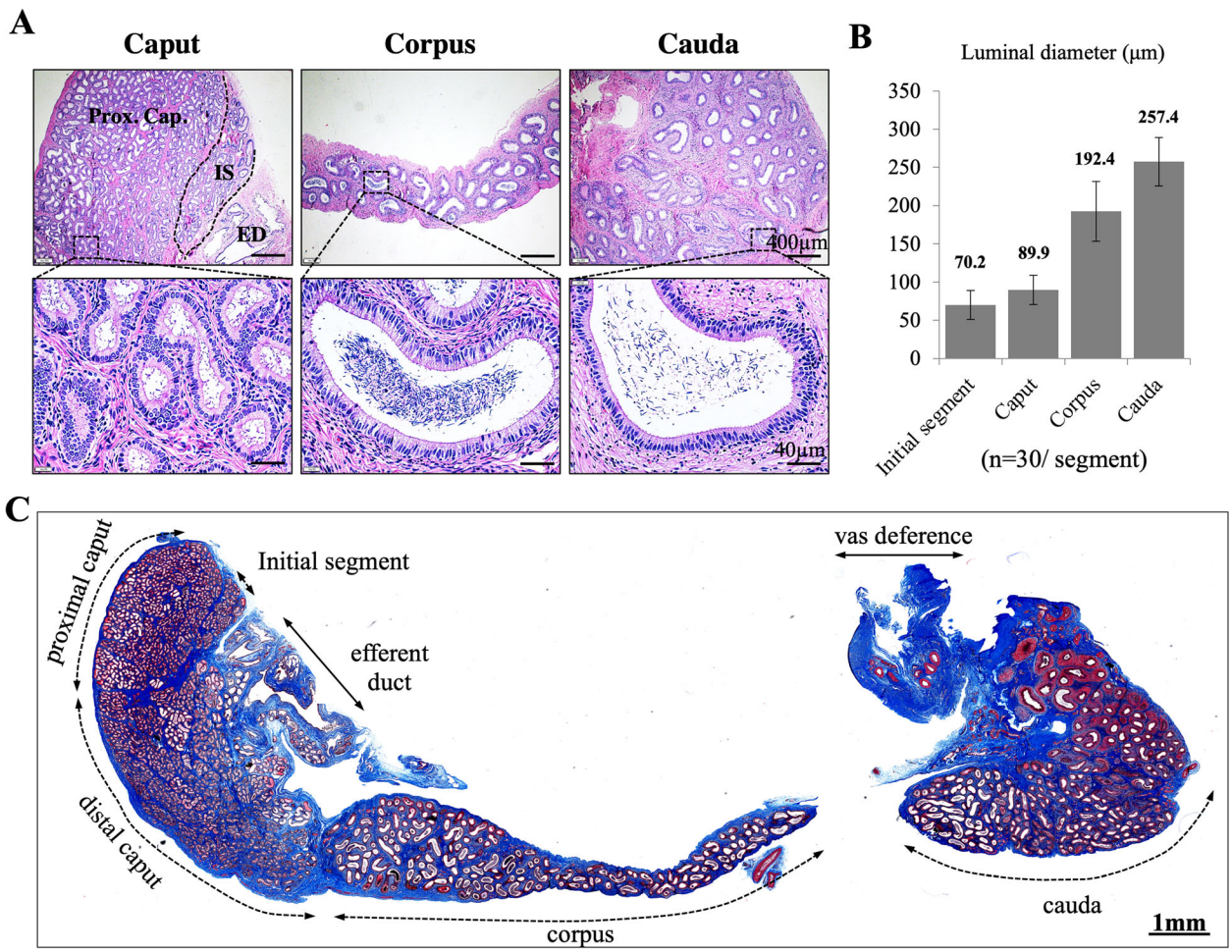

Fig. 1 General structures of pangolin testis and epididymis. **a** Similar to most known mammals, pangolin testis consisted of multi-layer spermatogenic cells surrounded in circle and formed the basic structure of testicular seminiferous tubules. Moreover, sertoli cells which is responsible for maintaining testicular structure is also present (labelled by SOX9 in green) in pangolin testis and showed a well-distributed pattern. **b** Pangolin epididymis showed an apparent compartmentalization separated by connective tissue that efferent duct (ED), initial segment (IS), caput, corpus and cadua epididymis can easily be distinguished. Magnified images indicated that pangolin epididymal lumen was consisted by single epithelium layer. **c** Quantification measurements showed the average luminal diameter of different epididymal lumen was 70.17 ± 18.9 μm, 89.87 ± 19.1 μm, 192.41 ± 39.2 μm, 257.36 ± 31.7 μm for initial segment, caput, corpus and cauda epididymis, respectively. **d** Masson's Trichrome stain which specifically illustrated the presence of connective tissue showed pangolin epididymis was enriched with fibrotic tissue. L: lumen, ED: efferent duct, IS: initial segment, prox. Caput: proximal caput. Representative images were presented. At least 30 lm per epididymal segment were measured

morphology and structure of pangolin sperm cells obtained from cauda epididymis. To our surprise, we observed a rod-shaped morphology of pangolin sperm head similar to that of avian, reptile (e.g. lizard) and amphibians (e.g. frog); quantitative analysis showed that the total length of pangolin sperm was measured as 60.7 ± 6.8 μm with 10.4 ± 1. μm, 9.9 ± 1. 4 μm, 40.4. ± 5. 8 μm for sperm head, mid-piece and sperm tail, respectively (Fig. 3a). Moreover, transmission electron micrograph showed similar to sperm structures of most mammals, pangolin sperm contained 9 + 2 pairs of axoneme (a) surrounded by dense fibers (df) and mitochondria (mt) at the mid-piece, distinct fibrous sheath (fs) surrounded the axoneme was also observed at the distal principal piece and sperm tail (end piece, Fig. 3b). Interestingly, besides typical rod-shaped sperm head, we also observed occasionally, a round−/oval-shaped sperm head (Fig. 3c, indicated with arrowheads). When we examined further in detail, the structure of the pangolin sperm head, we noticed that instead of double acrosome membranes (outer and inner) commonly described in rodent or other mammals [17], we observed a multiple bi-lamellar membrane structure present at the acrosome region of the pangolin sperm head (Fig. 4a). This observation was

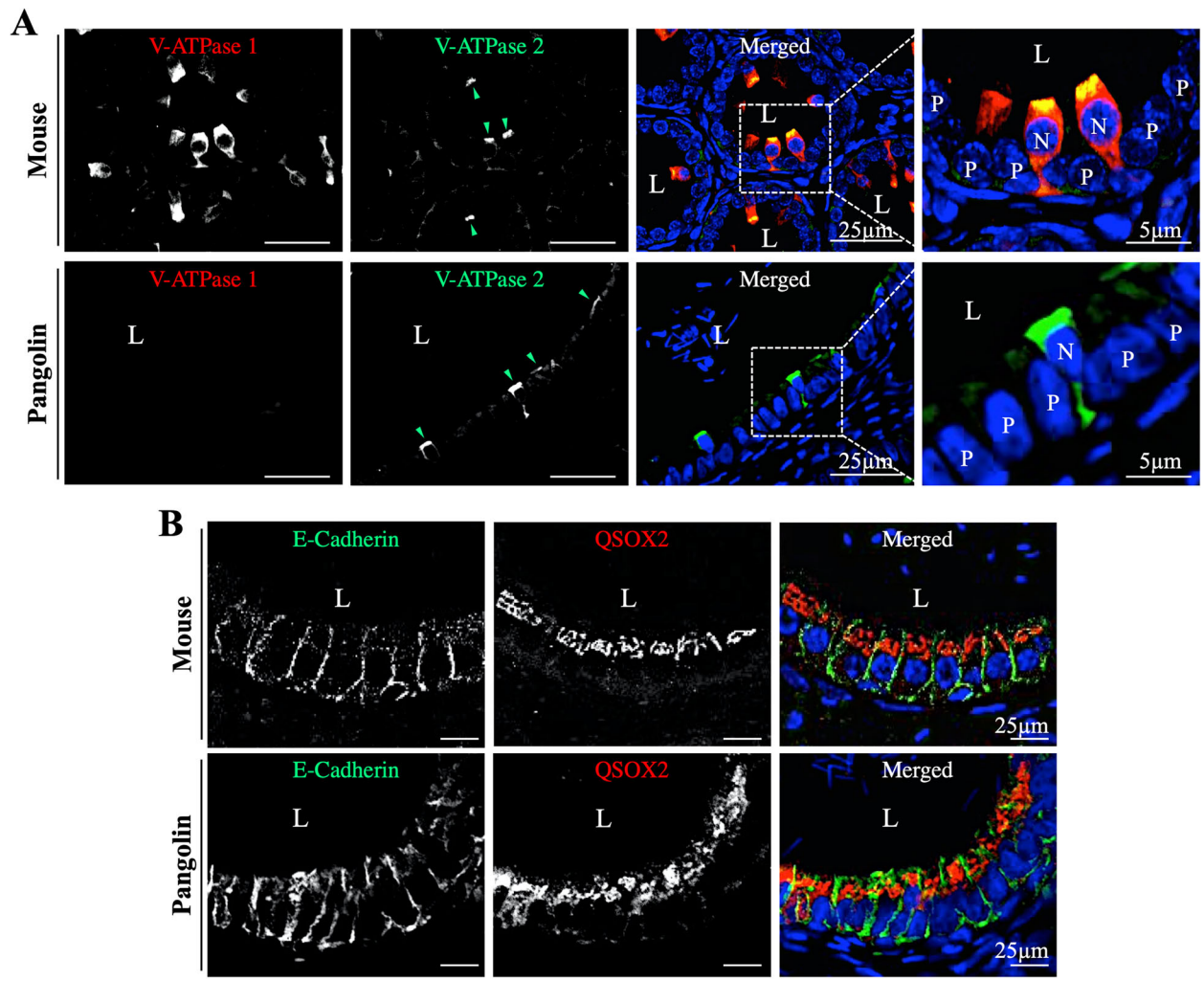

Fig. 2 V-ATPase subunit 2, but not subunit 1 was present in the pangolin epididymis. **a** When compared with mouse epididymis exhibited V-ATPase subunits 1and 2, we detected only V-ATPase subunit 2 present in the clear cells of the pangolin epididymis. **b** E-Cadherin (in green) which is known to maintain the polarity of epithelium is present at the lateral membrane of the pangolin epididymal epithelium; moreover, similar to our earlier observation in mouse, QSOX2 (in red), a protein critical for disulfide bond formation and sperm structure was also detected in the principal cells

further evidenced by cross-section of sperm head that onion-like multi-layer membrane structure was present (Fig. 4a, inset). Besides packed multi-layer sperm head membrane structure, we also observed a swollen acrosome (Fig. 4b) as described at early stage acrosome reacting sperm in other species [18]. Acrosome reaction was known to generate fusion vesicles formed by plasma membrane and outer acrosome membrane, we showed in Fig. 4c, similar fusion vesicles were detected at the acrosome (cell on the left, vesicles marked by asterisks) and likely to be released at completion of acrosome reaction (Fig. 4c, cell on the right), suggested a dynamic rearrangement of sperm head membrane can also occur at different stages of pangolin sperm cells.

Dynamic rearrangement of pangolin sperm head membrane coincided with the presence of tyrosine phosphorylated proteins

Capacitation and acrosome reaction are two important processes for sperm physiology to acquire the ability to fertilize the oocyte, to examine whether pangolin sperm has similar changes, we evaluated pangolin sperm acrosome status using a well-accepted PNA stain [19, 20]. As compared with mouse and chimpanzee sperm, we observed three distinct patterns of PNA staining in pangolin corresponded to well-characterized patterns of inactivated, capacitation and acrosome reacted sperm cells of other mammals (Fig. 5a) [19, 20]. The first pattern we detected was a triangle PNA positive structure

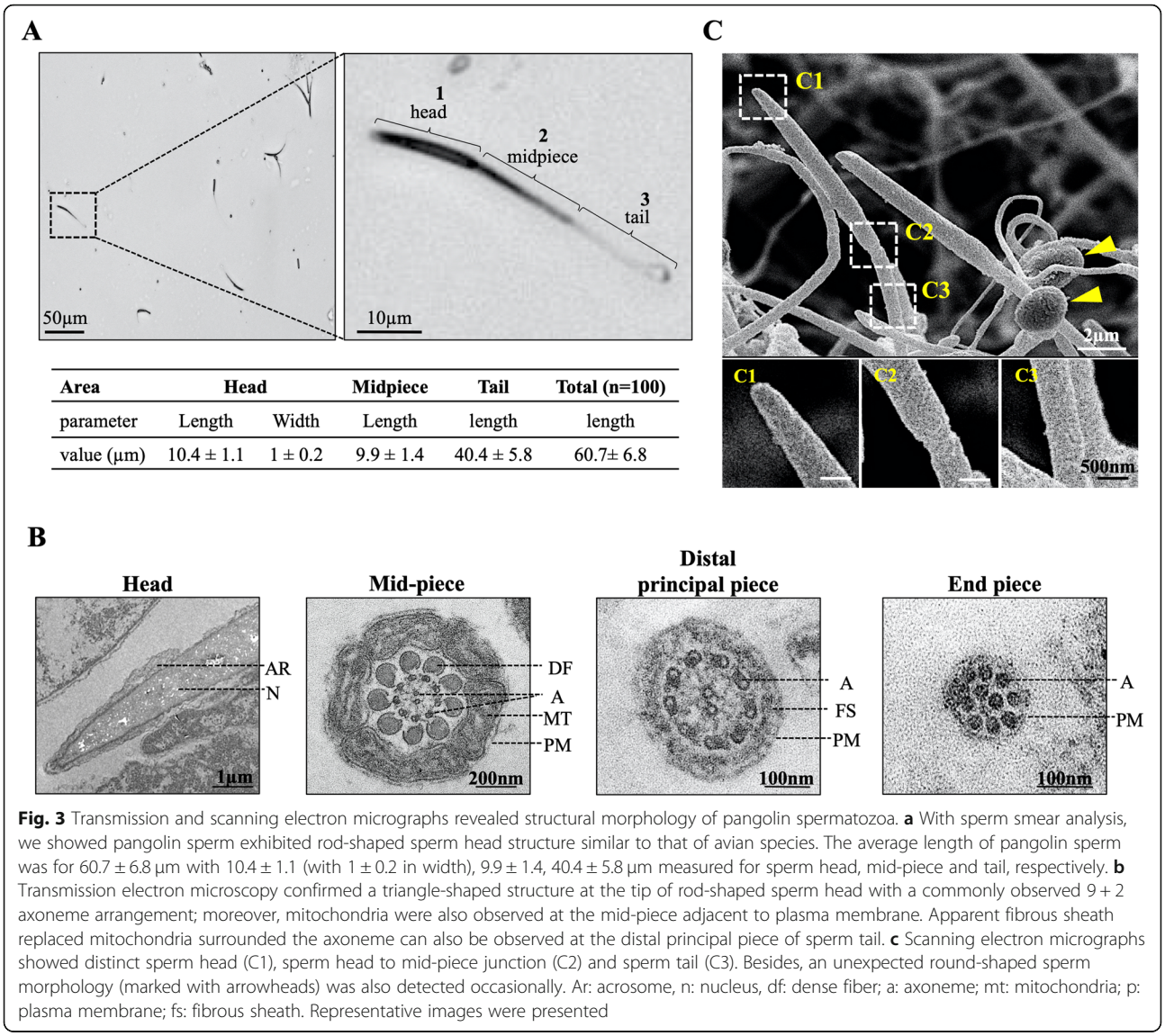

Area	Head		Midpiece	Tail	Total (n=100)
parameter	Length	Width	Length	length	length
value (μm)	10.4 ± 1.1	1 ± 0.2	9.9 ± 1.4	40.4 ± 5.8	60.7± 6.8

Fig. 3 Transmission and scanning electron micrographs revealed structural morphology of pangolin spermatozoa. **a** With sperm smear analysis, we showed pangolin sperm exhibited rod-shaped sperm head structure similar to that of avian species. The average length of pangolin sperm was for 60.7 ± 6.8 μm with 10.4 ± 1.1 (with 1 ± 0.2 in width), 9.9 ± 1.4, 40.4 ± 5.8 μm measured for sperm head, mid-piece and tail, respectively. **b** Transmission electron microscopy confirmed a triangle-shaped structure at the tip of rod-shaped sperm head with a commonly observed 9 + 2 axoneme arrangement; moreover, mitochondria were also observed at the mid-piece adjacent to plasma membrane. Apparent fibrous sheath replaced mitochondria surrounded the axoneme can also be observed at the distal principal piece of sperm tail. **c** Scanning electron micrographs showed distinct sperm head (C1), sperm head to mid-piece junction (C2) and sperm tail (C3). Besides, an unexpected round-shaped sperm morphology (marked with arrowheads) was also detected occasionally. Ar: acrosome, n: nucleus, df: dense fiber; a: axoneme; mt: mitochondria; p: plasma membrane; fs: fibrous sheath. Representative images were presented

(in green) at the tip of sperm head likely represent intact sperm acrosome (Fig. 5b, left image, 72%); the second pattern we observed exhibited punctate signals (indicated with arrowheads) aggregated at the apical tip of sperm head with additional homogeneous PNA signal appeared at the edge of the sperm head (indicated with arrows) (Fig. 5b, middle image, 19%); the third pattern showed remnant or weak PNA signal at the sperm head similar to those observed in rodent and primate species (Fig. 5b, right image, 9%). As no current information or protocol indicated sperm acrosome status or sperm capacitation status for pangolin, we here reported our observation and suggested that these patterns may represent, as in other mammals, three distinct stages of inactivated, capacitated and acrosome reacted sperm cells.

Sperm capacitation is characterized with increasing amount of tyrosine phosphorylation proteins present at the tail, we next examined whether tyrosine phosphorylation of proteins can also be detected in pangolin sperm. We applied anti-phospho-tyrosine (pTyrosin) antibody and observed that unlike in rodent or primate species showed the presence of tyrosine phosphorylated proteins at the sperm tail, we observed in pangolin sperm, tyrosine phosphorylated protein can be detected at both sperm mid-piece and tail (Fig. 5c, d). One interesting observation was that the emergency of tyrosine phosphorylated proteins was coincided with the rearrangement of PNA signal at the sperm head suggested that tyrosine phosphorylation occurred in pangolin sperm, and this increase amount of tyrosine phosphorylated proteins likely represent capacitation status of pangolin sperm as

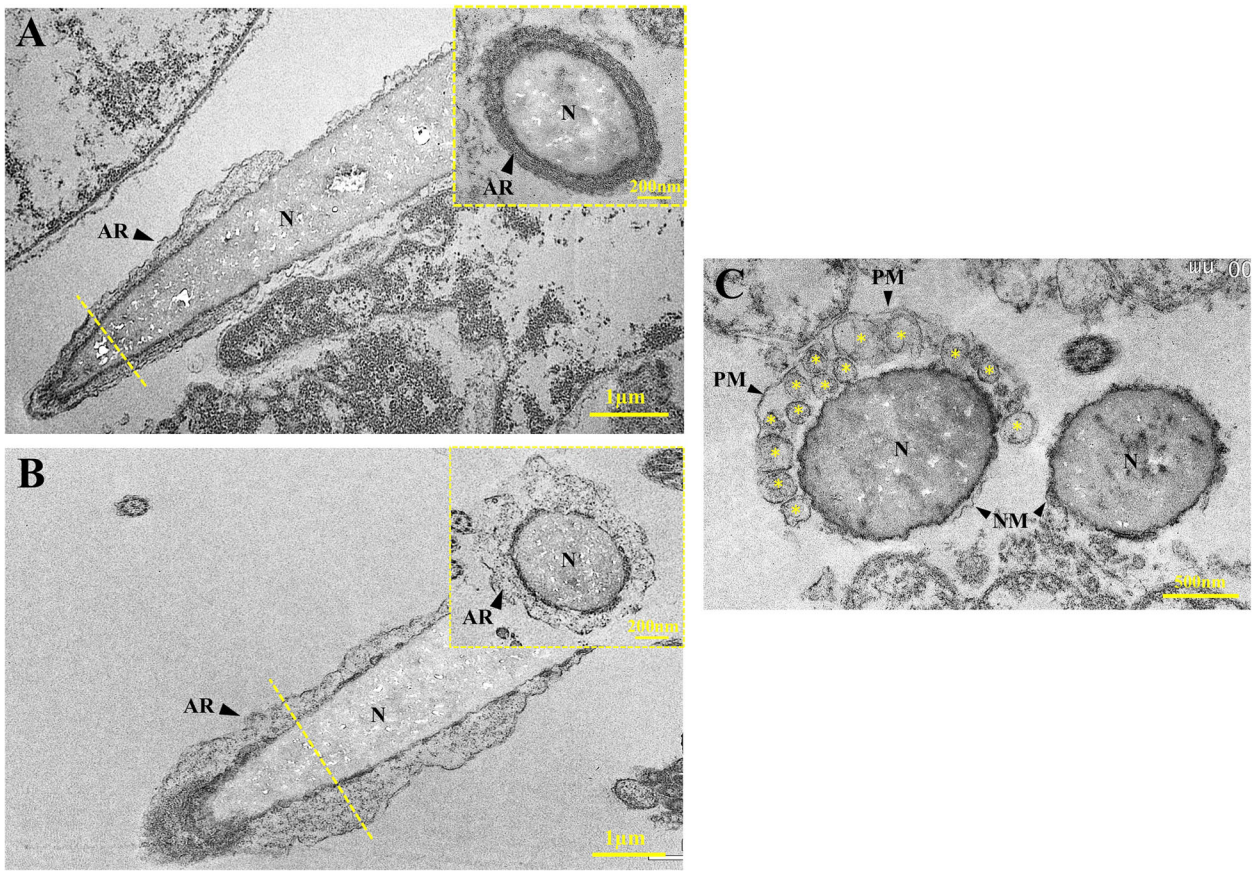

Fig. 4 Transmission electron micrographs demonstrated multi-layer membrane structural at pangolin sperm head. **a** We observed multiple membrane layers presented at the pangolin sperm head region; cross section of sperm head region (inset image) further confirmed this observation. **b** Acrosome swelling was observed likely representing acrosome reacting process as reported in other species. Cross section of sperm head showed an expansion of sperm acrosome. **c** Membrane fusion event was detected at the sperm head; fusion vesicles (marked with asterisks) can be detected underneath intact plasma membrane. The spermatozoa on the right likely represent acrosome reacted sperm with release plasma membrane and fusion vesicles. AR: acrosome, N: nucleus; PM: plasma membrane; NM: nuclear membrane; yellow dashed line illustrated the cross-section image observed in the inset figures

described in other species. Moreover, the co-occurrence of punctate PNA structure at the sperm head may indicate the dynamic reorganization of sperm head membrane upon capacitation in pangolin sperm (Fig. 5c, d).

Discussion

Breeding of wildlife or zoo captive animals is always challenging due to low number of individuals and limited knowledge to recreate natural housing and breeding conditions with appropriate feeding/nutrient formulation. Pangolins are an ant-eating nocturnal animals having both terrestrial (ground-dwelling) and arboreal (tree-climbing) living behavior, the terrestrial pangolin species, such as Formosan pangolins (*M. P. pentadactyla*) dig tunnels underground up to a depth of 3.5 m; in addition, they spend most of their hours in self-digging underground dwell during the daylight which makes less accessible for research purposes in terms of understand their reproductive parameters. Although many zoos or institutes keep pangolins in captivity, limited cases on successful breeding of captive pangolins have been reported [6, 21]. Experiences and knowledge from Sudan and Chinese pangolin showed that sexually mature pangolins should reach a body weight of at least 3 kg to achieve better success for breeding and the subsequent pregnancy [6, 10]. Despite pregnancy- related parameters, such as estrus cycle, gestation length and litter size have been studied, scarce information regarding male reproduction is available. In this study, we characterized for the first-time male reproductive tract of Formosan pangolin and reported rod-shaped pangolin spermatozoa with multi-layer acrosome membrane at the tip of sperm head. Although differences regarding membrane arrangements between pangolin sperm and other species

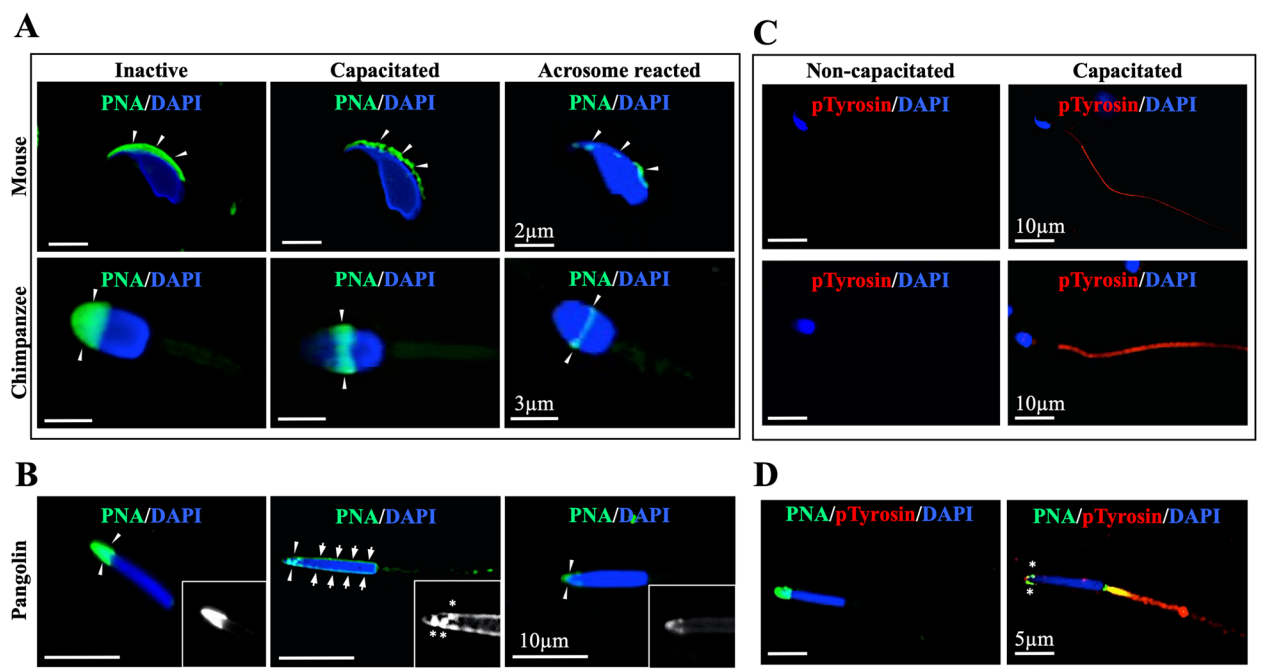

Fig. 5 Distinct patterns were observed for pangolin sperm acrosome and tail tyrosine phosphorylation status. **a** Dynamic rearrangement of sperm acrosome can be observed when mouse and chimpanzee (represent primate species) sperm cells were incubated in defined stimulation media, at these defined media, sperm capacitation and acrosome reaction can be induced and sperm acrosome (indicated with arrowheads) and its integrity can be observed by acrosome specific PNA staining. **b** Three distinct acrosome patterns were detected likely represent intact inactive sperm (left panel), acrosome reacting sperm (middle panel) and acrosome reacted sperm (right panel) as triangle-shaped, aggregated punctuated and weak diffused PNA stain were observed (marked with arrowheads). Moreover, rearrangement of sperm acrosome from the apical tip toward the edge of sperm head (marked with arrows) was also observed when aggregated punctuated PNA stain (marked with asterisks, inset image) was detected. **c** Increase protein tyrosine phosphorylation can be observed at sperm tail when mouse and chimpanzee (represent primate species) sperm cells were incubated in capacitation media. **d** Two distinct patterns when anti-phosphotyrosine antibody was used to demonstrate protein tyrosine phosphorylation status of pangolin sperm. The first pattern showed no detection of signal at the sperm tail with homogenous PNA staining pattern (in green) present at the sperm head (left panel); another pattern showed strong signal throughout sperm mid-piece and sperm tail (in red) with PNA stain aggregated as punctuated signal at the tip of sperm head (in green, marked with asterisks). Moreover, we detected PNA signal occasionally present at the sperm mid-piece overlapping with phosphotyrosine signal

were reported here, pangolin sperm head contained lectin PNA at the acrosome region as described in other mammals [19, 20]. The observed redistribution and punctuated aggregation of PNA at pangolin sperm head likely represent capacitation and acrosome reaction physiological status as reported in other mammals [17, 18, 20]. Moreover, we also demonstrated that this redistribution of acrosome content was coincided with increased protein tyrosine phosphorylation at the sperm mid-piece and tail suggesting sperm capacitation-induced tyrosine phosphorylation and sperm head membrane rearrangement reported in other mammals may also exist in pangolin [19, 20, 22].

It has been shown in rodent species that acidic luminal pH in the epididymis contributes to the maintenance of sperm in quiescent during their maturation and storage in the epididymis [15]. Earlier studies also indicated that V-ATPase, a highly conserved proton channel is responsible for regulating luminal pH in the epididymis [23]. The presence of V-ATPase subunit 2 in pangolin epididymis indicated that regulation of proton secretion and the maintenance of acidic luminal pH may also be important for pangolin sperm physiology. Despite V-ATPase is composed of 13 distinct subunits with wide-ranged tissue distribution, two highly homologous 56 kDa isoforms of the subunit B, ATP6V1B1 (B1) and ATP6V1B2 (B2) have been identified in the epididymis of human, rodent, pig and bat [12, 23–26].. Unlike human epididymis where V-ATPase B1 and B2 subunits located at the restricted apical membrane and microvilli (V-ATPase B1) or intracellular structure (V-ATPase B2), respectively [24, 27], we did not detect the presence of V-ATPase B1 in the pangolin epididymis, nevertheless, we observed V-ATPase B2 exhibited apical –enriched cellular localization rather than homogenous intracellular distribution, likely representing functional compensation as described by Da Silva et al. in V-ATPase B1 subunit deficiency mice [27].

Rearrangement of sperm head membrane upon sperm capacitation and acrosome reaction facilitate relocation of essential proteins for sperm-egg recognition and fusion [17, 18, 28, 29]. Currently, no defined medium can be used to induce pangolin sperm to a specific defined physiological status (i.e. capacitated or acrosome reacted); it is therefore difficult to correlate the observed patterns to their actual physiological status; however, defined sperm activation stages have ben well-established for mouse and chimpanzee sperm; therefore, to compare the similarities and differences between observed sperm membrane patterns with defined sperm activation stages, mouse sperm cells were used. We demonstrated that pangolin sperm formed punctuated aggregation at the apical sperm head, and this rearrangement coincided with increased tyrosine phosphorylation on sperm midpiece and tail likely representing "sperm capacitation" status as reported in other species [20, 22, 30, 31]; moreover, acrosome swelling and disappearance of acrosome content PNA were also detected likely representing "sperm acrosome reacting and acrosome reacted" status as reported in other mammals [18, 19, 30]. Based on above-mentioned observation and morphological evidence from TEM, we considered pangolin sperm could undergo capacitation and acrosome reaction processes with similar membrane rearrangement as reported in other species.

Conclusions

In conclusion, pangolin is an endangered species with many unknown reproductive characterizations, we reported for the first time in this study, male reproductive parameters of Formosan pangolin, especially unique presence and distribution of epididymal proton regulatory channel, V-ATPase 2 and three dynamic sperm head membrane reorganization. Our findings would achieve better understanding on sperm membrane changes of Formosan pangolin and their reproduction tract, although this may not directly or immediately improve breeding success of zoo captive population, but will certainly benefit the understanding of reproduction properties in general of this endangered species.

Methods

Chemicals, reagents, antibodies

Chemicals and reagents were obtained from Sigma-Aldrich (St. Louis, MO, USA) unless otherwise stated. For sperm acrosome integrity evaluation, peanut agglutinin (PNA) (*Arachis hypogaea*) conjugated with Alexa 488 fluorophore was purchased from Invitrogen (L21409, Invitrogen/Life Technologies, Carlsbad, CA, USA). Rabbit polyclonal anti-quiescin sulfhydryl oxidase 2 (QSOX2, Ab121376), polyclonal anti-V-ATPase B1 (Ab118003), polyclonal anti-V-ATPase B2 (Ab73404) were obtained from Abcam (Cambridge, UK), rabbit polyclonal anti-V-ATPase 1//2 (SC-20943, detect both B1 and B2 subunits) were purchased from Santa Cruz Biotechnology (Dallas, TX, USA), mouse monoclonal anti-E Cadherin (#14472S) was acquired from Cell Signaling (Beverly, MA, USA), mouse monoclonal anti-Phosphotyrosine (#05–1050) antibody was purchased from Merk/Millipore (Burlington, MA, USA). All secondary antibodies were obtained from Jackson ImmunoResearch (West Grove, PA, USA).

Animals and sperm acquisition

To compare the similarity and differences, 3 Caesarean Derived-1 (ICR, CD1) mice were used and were obtained from National Laboratory Animal Center, Taiwan and were acclimatized (3 mice/cage) for 1 week prior to experiments. Ethics approval and sample collections of mouse materials were performed and supervised by the approved veterinarians throughout the study and followed the regulation and approval of animal welfare committee of National Taiwan University (#NTU106-EL-00124). The animal housing room was kept at a constant temperature (22–24 °C) with a 12 h alternating light-dark cycle. Animals were given water and standard mice lab chow (Oriental yeast, Tokyo, JP) ad libitum. Animals were euthanized by CO_2 chambers followed by cervical dislocation before sample collection. For pangolin sample acquisition, we collected epididymes and sperm samples from deceased individuals ($n = 5$) during routine visit and necropsy at Taipei zoo during 2017–2018. Due to small volume (< 5 μl/ ejaculate) and high viscosity of pangolin semen ejaculate, it was difficulty to acquire sufficient amount of sperm cells for in vitro evaluation, we therefore followed standard procedures similar to that of rodent species to obtain swim out pangolin sperm cells from the epididymis. In short, epididymes were acquired from deceased individuals during necropsy, and were carefully separated from fat and overlying connective tissue immediately on a temperature- controlled stage. Epididymal sperm cells were allowed to swim out for 10 min in a freshly- prepared pre-warmed Ham's F10 medium. For morphological evaluation, standard papanicolaou (PAP) and POPE's staining procedures were carried out as previously described [20, 32–34], and 200 sperm cells were evaluated. For acrosome evaluation, sperm cells were fixed in 4% paraformaldehyde (PFA) at room temperature (RT) for 1 h and analysed as described below.

Tissue preparation and Histochemistry staining

Both testis and epididymis were obtained during necropsy examination and were fixed in 10% neutralized formalin for overnight on shaker. For histochemistry

staining, paraffin-embedded testis and epididymis were sectioned at 10 μm and used for standard histochemistry procedures [35]. After de-paraffinization procedures via xylene and ethanol gradients (100–80%), tissue sections were subjected to hematoxylin and eosin (H&E) stain for general morphological analysis and Masson's trichrome stain for the evaluation of fibrotic tissue.

Indirect Immunofluorescent (IFA)

Indirect immunofluorescent staining was carried out to evaluate sperm tyrosine phosphorylation, acrosome integrity, as well as the presence and the distribution of specific marker proteins in male reproductive tract. Based on published literatures, in current study, sperm capacitation status was assessed by the emergency of phosphotyrosine signal at the sperm tail [22] and acrosome integrity was evaluated by the presence of lectin PNA at the sperm head as previously described [20]. Briefly, fixed spermatozoa were washed and resuspended in PBS; 20 μl of sperm suspension was added onto Superfrost Plus Microscope Slides (Thermo Scientific/Invitrogen), and spermatozoa were allowed to attach to the slide for 10 min, unbound sperm cells were removed with PBS and sperm smears were dried and keep at − 20 °C until used. Antibody incubations were carried out by using anti- phosphotyrosine (1:250) or peanut agglutinin (PNA) conjugated with Alexa 488 at 2 mM for 1 h at RT.

To evaluate and to compare the presence and distribution of testicular and epididymal marker proteins in pangolin reproductive tract, standard IFA procedures were followed as described earlier [13]. Ten μm paraffin-embedded tissue sections were de-paraffinized as above-mentioned, antigen retrieval was carried out by submerging slides with 10 mM citrate buffer (pH 6.0) and heated up to 95 °C for 2 times, 5 min. Tissue sections were subsequently permeabilized with either 100% methanol at − 20 °C for 10 min or with 0.1% Triton X 100 for 2 h at RT. After blocked with 5% BSA for 60 min at RT, primary antibody incubation (V-ATPase1, 2, 1/2–1:200; QSOX2–1:200; E-Cadherin- 1:100) was carried out with O/N incubation at 4 °C. After intense washed, sections were subsequently incubated with secondary antibodies for 1.5 h at RT. As for negative controls, each immunoreaction was accompanied by a reaction omitting the primary antibody. Nuclei were counter stained with 4′,6-diamidino-2-phenylindole (DAPI) (Vectashield H-1200, Vector Laboratories, Peterborough, UK), and slides were then sealed with nail polish. For the sperm capacitation and acrosome integrity evaluation, at least 200 spermatozoa were examined, for protein distribution in the testis and epididymis, at least 10 frames were evaluated in each sample under Olympus IX83 epifluorescence microscopy (Olympus, Tokyo, JP) and analyzed with either ImageJ (NIH; http://rsb.info.nih.gov/ij/) or Cellsens software (Olympus).

Transmission and scanning Electron microscopy

For transmission electron micrograph (TEM) evaluation, sperm cells were fixed overnight at 4 °C in Karnovsky (contains 2% (v/v) paraformaldehyde and 2.5% (v/v) glutaraldehyde diluted in cacodylate buffer) fixative. Pellets were washed with 0.1 M Na-cacodylate (pH 7.4) and post-fixed with 1% osmium tetraoxide in 0.1 M Na-cacodylate (pH 7.4) for 1 h. After washing with milli-Q H_2O, pellets were incubated with 2% (w/v) uranylacetate for 1 h. Fixed pellets were subsequently dehydrated in graded series of acetone (50–100%) and embedded in Durcupan ACM resin (Fluka, Bachs, Switzerland). Ultrathin sections of 70–80 nm were obtained on a Ultramicrotome (Leica EM UC7, Watzler, Germany), and studied using TEM (JEM-1200EX II, Jeol USA, Peabody, MA, USA). For scanning electron microscopy (SEM, JSM-6510LV, Jeol USA, Peabody, MA, USA), same procedures as described for TEM were followed. Sperm pellets were dried in a critical point dryer (Leica, EM CPD300, Watzler, Germany) and gold coated by Sputter Coater (SPI-MODULE, West Chester, PA, USA) for final visualization.

Abbreviations

DPAI: 4′,6-diamidino-2-phenylindole; HE: Hematoxylin and eosin; PAP: Papanicolaou; PFA: Paraformaldehyde; PNA: Peanut agglutinin; QSOX2: Quiescin sulfhydryl oxidase 2; RT: Room temperature; SEM: Scanning electron micrograph; TEM: Transmission electron micrograph; V-ATPase: Vacuolar type H^+ – ATPase

Acknowledgements

Not applicable.

Authors' contributions

YJC, JFY, TEW, YSW and TYC performed sample collections and contributed to all experimental data presented in this manuscript; YJC, JFY, SCC and PST conceived and designed the experiments. YJC, JFY and PST wrote and constructed the manuscript. All authors have read and approve this article at submission.

Funding

This work was supported by grants from the ministry of Science and Technology, Taiwan (grant #105–2628-B-002-022-MY3 for PSJ TSAI) and general financial support from the Taipei City Hall for Taipei Zoo, Taiwan.

Availability of data and materials

The isolation and purification protocols and materials used that were analyzed in current study, as well as initial raw data collected, are available from the corresponding author on reasonable request.

Ethics approval and consent to participate

Ethics approval and sample collections were performed and supervised by the approved veterinarians throughout the study. Material collections from the animals followed the regulation and approval of animal welfare committee of National Taiwan University (#NTU106-EL-00124), and was monitored under the guidance of the animal welfare committee of Taipei Zoo. Consent was obtained for the samples to be collected at the Taipei Zoo.

Consent for publication
Not applicable.

Competing interests
All authors declare no conflict of interests that could prejudice the impartiality of the research reported.

Author details
[1]Reproductive Science Lab, Conservation and Research Center, Taipei Zoo, 30 Xinguang Road, Section 2, Wenshan, Taipei 11656, Taiwan. [2]Graduate Institute of Veterinary Medicine, National Taiwan University, No. 1, Sec. 4, Roosevelt Rd, 10617 Taipei, Taiwan. [3]Animal medical center, Taipei Zoo, 30 Xinguang Road, Section 2, Wenshan, Taipei 11656, Taiwan. [4]Department of Veterinary Medicine, National Taiwan University, No. 1, Sec. 4, Roosevelt Rd, 10617 Taipei, Taiwan. [5]Research Center for Developmental Biology and Regenerative Medicine, National Taiwan University, No. 1, Sec. 4, Roosevelt Rd, 10617 Taipei, Taiwan.

Received: 22 July 2020 Accepted: 15 October 2020
Published online: 27 October 2020

References

1. Da S. Order Pholidota. In: RD WDE, editor. Mammal species of the world: a taxonomic and geographic reference. 2nd ed. Washington, DC: Smithsonian Institution Press; 1993. p. 415.
2. Prakash Kumar V, Rajpoot A, Srivastav A, Nigam P, Kumar V. A M, Prakash Goyal S: phylogenetic relationship and molecular dating of Indian pangolin (Manis crassicaudata) with other extant pangolin species based on complete cytochrome b mitochondrial gene. Mitochondrial DNA A DNA Mapp Seq Anal. 2018;29(8):1276–83.
3. Wu SBMG, Tang M, Chen H, Liu NF. The status and conservation strategy of pangolin resource in China. J Nat Resour. 2002;17(2):174–80.
4. Challender DWS, Hoffmann M, Hoffmann R, Scott J, Robinson JE, Cremona P, Hilton-Taylor C, Jenkins RKB, Malsch K, Conde D, et al. Criteria for CITES species protection. Science. 2019;364(6437):247–8.
5. Challender D, Baillie, J., Ades, G., Kaspal, P., Chan, B., Khatiwada, A., Xu, L., Chin, S., Nash, H. Hsieh, H.: Manis pentadactyla. The IUCN Red List of Threatened Species. 2014:e:T12764A5222544.
6. Zhang F, Yu J, Wu S, Li S, Zou C, Wang Q, Sun R. Keeping and breeding the rescued Sunda pangolins (Manis javanica) in captivity. Zoo Biol. 2017;36(6):387–96.
7. Hua L, Gong S, Wang F, Li W, Ge Y, Li X, Hou F. Captive breeding of pangolins: current status, problems and future prospects. ZooKeys. 2015;507:99–114.
8. Zhang F, Wu S, Zou C, Wang Q, Li S, Sun R. A note on captive breeding and reproductive parameters of the Chinese pangolin, Manis pentadactyla Linnaeus, 1758. ZooKeys. 2016;618:129–44.
9. Zhang F, Yu Y, Yu J, Wu S, Li S, Wang Q, Min Y, Sun R. Reproductive behavior of the captive Sunda pangolin (Manis javanica Desmarest, 1822). Zoo Biol. 2020;39(2):65–72.
10. Chin SC, Lien CY, Chan YT, Chen CL, Yang YC, Yeh LS. Monitoring the gestation period of rescued Formosan pangolin (Manis pentadactyla pentadactyla) with progesterone radioimmunoassay. Zoo Biol. 2012;31(4):479–89.
11. Chen DYLC, Yu CB. Evaluation of pangolin parturient time. Res Dev Mark. 2000;16:287.
12. Shum WW, Ruan YC, Da Silva N, Breton S. Establishment of cell-cell cross talk in the epididymis: control of luminal acidification. J Androl. 2011;32(6):576–86.
13. Wang TE, Li SH, Minabe S, Anderson AL, Dun MD, Maeda KI, Matsuda F, Chang HW, Nixon B, Tsai PJ. Mouse quiescin sulfhydryl oxidases exhibit distinct epididymal luminal distribution with segment-specific sperm surface associations. Biol Reprod. 2018;99(5):1022–33.
14. Andersson AM, Edvardsen K, Skakkebaek NE. Expression and localization of N- and E-cadherin in the human testis and epididymis. Int J Androl. 1994;17(4):174–80.
15. Breton S, Nair AV, Battistone MA. Epithelial dynamics in the epididymis: role in the maturation, protection, and storage of spermatozoa. Andrology. 2019;7(5):631–43.
16. Battistone MA, Merkulova M, Park YJ, Peralta MA, Gombar F, Brown D, Breton S. Unravelling purinergic regulation in the epididymis: activation of V-ATPase-dependent acidification by luminal ATP and adenosine. J Physiol. 2019;597(7):1957–73.
17. Tsai PS, Brewis IA, van Maaren J, Gadella BM. Involvement of complexin 2 in docking, locking and unlocking of different SNARE complexes during sperm capacitation and induced acrosomal exocytosis. PLoS One. 2012;7(3):e32603.
18. Sosa CM, Zanetti MN, Pocognoni CA, Mayorga LS. Acrosomal swelling is triggered by cAMP downstream of the opening of store-operated calcium channels during Acrosomal exocytosis in human sperm. Biol Reprod. 2016;94(3):57.
19. Cheng F, Fazeli A, Voorhout W, Marks A, Bevers M, Colenbrander B. Use of peanut agglutinin to assess the acrosomal status and the zona pellucida-induced acrosome reaction in stallion spermatozoa. J Androl. 1996;17(6):674–82.
20. Yu JF, Lai YH, Wang TE, Wei YS, Chang YJ, Li SH, Chin SC, Joshi R, Chang HW, Tsai PS. The effects of type I collagenase on the degelification of chimpanzee (pan troglodytes) semen plug and sperm quality. BMC Vet Res. 2018;14(1):58.
21. Zhang F, Wu S, Yang L, Li S, Zhang L. A Sunda pangolin's cub with malformation was born in captivity. J Econ Animal. 2013;17(2):105–8.
22. Naresh S, Atreja SK. The protein tyrosine phosphorylation during in vitro capacitation and cryopreservation of mammalian spermatozoa. Cryobiology. 2015;70(3):211–6.
23. Brown D, Breton S. H(+)V-ATPase-dependent luminal acidification in the kidney collecting duct and the epididymis/vas deferens: vesicle recycling and transcytotic pathways. J Exp Biol. 2000;203(1):137–45.
24. Breton S, Smith PJ, Lui B, Brown D. Acidification of the male reproductive tract by a proton pumping (H+)-ATPase. Nat Med. 1996;2(4):470–2.
25. Castro MM, Kim B, Hill E, Fialho MC, Puga LC, Freitas MB, Breton S, Machado-Neves M. The expression patterns of aquaporin 9, vacuolar H(+)-ATPase, and cytokeratin 5 in the epididymis of the common vampire bat. Histochem Cell Biol. 2017;147(1):39–48.
26. Park YJ, Kim JH, Kim HY, Park HB, Choe J, Kim GW, Baek SY, Chung HJ, Park YJ, Kim B. The expression and localization of V-ATPase and cytokeratin 5 during postnatal development of the pig epididymis. Asian-Australas J Anim Sci. 2020;33(7):1077–86.
27. Da Silva N, Shum WW, El-Annan J, Paunescu TG, McKee M, Smith PJ, Brown D, Breton S. Relocalization of the V-ATPase B2 subunit to the apical membrane of epididymal clear cells of mice deficient in the B1 subunit. Am J Phys Cell Phys. 2007;293(1):C199–210.
28. Gadella BM, Boerke A. An update on post-ejaculatory remodeling of the sperm surface before mammalian fertilization. Theriogenology. 2016;85(1):113–24.
29. Gadella BM, Tsai PS, Boerke A, Brewis IA. Sperm head membrane reorganisation during capacitation. Int J Dev Biol. 2008;52(5–6):473–80.
30. Gadella BM, Rathi R, Brouwers JF, Stout TA, Colenbrander B. Capacitation and the acrosome reaction in equine sperm. Anim Reprod Sci. 2001;68(3–4):249–65.
31. Katoh Y, Takebayashi K, Kikuchi A, Iki A, Kikuchi K, Tamba M, Kawashima A, Matsuda M, Okamura N. Porcine sperm capacitation involves tyrosine phosphorylation and activation of aldose reductase. Reproduction. 2014;148(4):389–401.
32. Pope CE, Zhang YZ, Dresser BL. A simple staining method for evaluating Acrosomal status of cat spermatozoa. J Zoo Wildlife Med. 1991;22:87–95.
33. Kruger TFAS, Simmons KF, Swanson RJ, Brugo SS, Acosta AA. A quick, reliable staining technique for human sperm morphology. Arch Androl. 1987;18(3):275–7.
34. Henkel RSG, Sturmhoefel A, Hipler UC, Zermann DH, Menkveld R. Comparison of three staining methods for the morphological evaluation of human spermatozoa. Fertil Steril. 2008;89(2):449–55.
35. Kuo YW, Joshi R, Wang TE, Chang HW, Li SH, Hsiao CN, Tsai PJ. Identification, characterization and purification of porcine Quiescin Q6-Sulfydryl oxidase 2 protein. BMC Vet Res. 2017;13(1):205.

Publisher's Note